BIOCHEMISTRY
including biophysical chemistry & molecular biology

Article

pubs.acs.org/biochemistry

Properties of Membrane-Incorporated WALP Peptides That Are Anchored on Only One End

Johanna M. Rankenberg,[†] Vitaly V. Vostrikov,[†] Denise V. Greathouse,[†] Christopher V. Grant,[‡] Stanley J. Opella,[‡] and Roger E. Koeppe, II*,[†]

[†]Department of Chemistry and Biochemistry, University of Arkansas, Fayetteville, Arkansas 72701, United States

[‡]Department of Chemistry and Biochemistry, University of California, San Diego, La Jolla, California 92093, United States

Supporting Information

ABSTRACT: Peptides of the "WALP" family, acetyl-GWW$(LA)_nLWWA$-[ethanol]amide, have proven to be opportune models for investigating lipid−peptide interactions. Because the average orientations and motional behavior of the N- and C-terminal Trp (W) residues differ, it is of interest to investigate how the positions of the tryptophans influence the properties of the membrane-incorporated peptides. To address this question, we synthesized acetyl-GGWW-$(LA)_n$-ethanolamide and acetyl-$(AL)_n$WWG-ethanolamide, in which n = 4 or 8, which we designate as "N-anchored" and "C-anchored" peptides, respectively. Selected ^2H or ^{15}N labels were incorporated for solid-state nuclear magnetic resonance (NMR) spectroscopy. These peptides can be considered "half"-anchored WALP peptides, having only one pair of interfacial Trp residues near either the amino or the carboxyl terminus. The hydrophobic lengths of the (n = 8) peptides are similar to that of WALP23. These longer half-anchored WALP peptides incorporate into lipid bilayers as α-helices, as reflected in their circular dichroism spectra. Solid-state NMR experiments indicate that the longer peptide helices assume defined transmembrane orientations with small non-zero average tilt angles and moderate to high dynamic averaging in bilayer membranes of 1,2-dioleoylphosphatidylcholine, 1,2-dimyristoylphosphatidylcholine, and 1,2-dilauroylphosphatidylcholine. The intrinsically small apparent tilt angles suggest that interactions of aromatic residues with lipid headgroups may play an important role in determining the magnitude of the peptide tilt in the bilayer membrane. The shorter (n = 4) peptides, in stark contrast to the longer peptides, display NMR spectra that are characteristic of greatly reduced motional averaging, probably because of peptide aggregation in the bilayer environment, and CD spectra that are characteristic of β-structure.

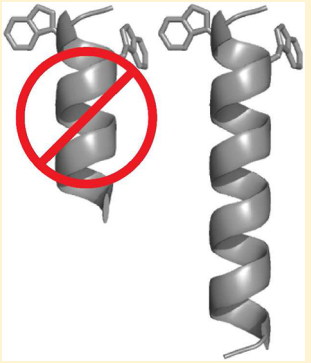

Model peptides have proven to be useful for describing the details of protein−lipid interactions in lipid bilayer membranes. For example, WALP and related peptides have been studied extensively to determine their behavior and positioning in lipid bilayers of varying thickness. WALP peptides, originally developed using gramicidin A channels as inspiration,[1] traditionally have contained two Trp residues on either side of a hydrophobic, helical core composed of alternating Leu and Ala residues, yielding the sequence pattern acetyl-GWWL$(AL)_n$WWA-amide (with n typically between 4.5 and 12). In proteins associated with biological membranes, such as photosynthetic reaction centers or potassium channels,[2,3] aromatic as well as charged amino acid side chains are often located at or near the membrane−water interfaces. The interfacial amino acid residues help to anchor the proteins in specific orientations within the bilayer. It follows that the aromatic Trp residues are key constituents of WALP model peptides, because they are the only residues available to restrict transbilayer movement or specify a particular tilt angle for the peptide helix.[4]

Previous studies have addressed the concept of hydrophobic mismatch between WALP (or related peptides) and lipid bilayer membranes.[4−6] The lipid bilayer thickness and the peptide hydrophobic length, defined as the distance between the Trp residues on either side of the Leu-Ala core, affect the lipid phase behavior and may influence the peptide orientation in cases where the bilayer phase is maintained. A remarkable and somewhat surprising recent finding[7] has revealed that peptides having only single Trp residues on both ends respond more systematically to changes in the lipid bilayer thickness than do peptides having pairs of Trp residues on both ends. Several methods have been employed to determine WALP or WALP-like peptide orientations within hydrated, oriented model lipid bilayer membranes. The measurements have included circular dichroism (CD) and infrared spectroscopy,[1,8] as well as solid-state nuclear magnetic resonance (NMR)[4,7,9−11] and fluorescence quenching,[12,13] along with molecular modeling.[9,11,14−16] The solid-state NMR methods have included the ^2H NMR-based geometric analysis of labeled alanines (GALA)[4,17] and the ^{15}N NMR-based polarization inversion with spin exchange at magic angle (PISEMA).[18,19] In several direct comparisons, the ^{15}N and ^2H methods have shown remarkable agreement.[7,10,20] More recently, considerations of ensemble dynamics[21] or multiple parameters for treating dynamics have been incorporated into the analysis.[7,9,14,16,20]

Received: May 31, 2012
Published: November 21, 2012

Here we describe the independent anchoring properties of Trp residues when they are present at only one end of a membrane-spanning peptide (Figure 1). Previous experiments

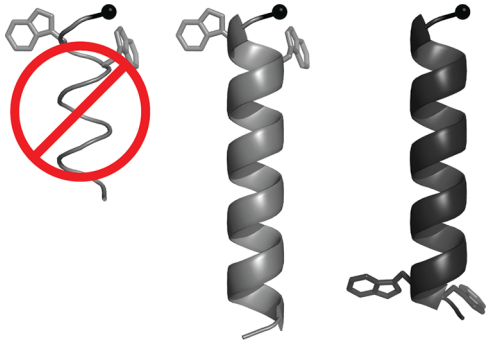

Figure 1. Schematic ribbon models for hydrophobic peptides of 11 or 19 residues, with two Trp residues near the N-terminus (lighter gray) or near the C-terminus (darker gray). The longer peptides could span a lipid bilayer membrane as α-helices, whereas the shorter peptides could span only approximately one leaflet of a bilayer. Nevertheless, the shorter peptides are not helical under such conditions.

have compared the influence of one- and two-Trp anchors,[7] when present on both ends of a WALP or WALP-like peptide. The presence or absence of interfacial Trp residues in specific N-proximal or C-proximal positions has the potential to affect the peptide dynamics as well as the preferred helix orientation. The presence of Trp residue(s) on (only) one side of a membrane sequence, without any anchor residues on the other side, offers a means to investigate the properties of peptides that are "held" on only one end. For this purpose, we have developed "single-end" anchored WALP peptides, which we henceforth designate as "single-anchored". Each peptide incorporates one pair of Trp residues adjacent to a string of either four or eight Leu-Ala repeating units, namely $(LA)_n$ in which n is four or eight. In this design, the C-anchored $(AL)_nWWG$ and N-anchored $GGWW(LA)_n$ peptides each retain two Trp residues near one end (Figure 1). As is true for other WALP and GWALP peptides, the termini are blocked with acetyl and ethanolamide groups, so that charged ends are avoided.

Using CD and solid-state NMR methods, we have characterized the folding, orientation, and dynamic properties of the single-end N- and C-anchored peptides, in DLPC, DMPC, and DOPC bilayer membranes. The shorter $(LA)_4$-containing peptides were found to exhibit β-structure and very slow dynamics, which we attribute to aggregation. For the $(LA)_8$-containing peptides, well-resolved ^2H and ^{15}N NMR resonances are observed and allow a detailed analysis of peptide orientation and dynamics.[20] Together, the results provide useful comparisons with other membrane-spanning peptides that appear to be anchored on only one side of a bilayer.[22] We find that the N- or C-anchored peptides of sufficient length tend to span the bilayer as helices with small tilt angles and extensive dynamics. Shorter peptides, whose lengths are similar to the thickness of a lipid monolayer, seem not to span the half-bilayer leaflet but instead adopt β-structure and aggregate.

MATERIALS AND METHODS

Materials. Isotope-enriched amino acids (^2H and ^{15}N) and ^2H-depleted water were from Cambridge Isotope Laboratories (Andover, MA). Commercial L-alanine-d_4 was Fmoc-protected using Fmoc-ON-succinimide as described previously.[23] Unlabeled Fmoc-amino acids and preloaded Wang resin were obtained from Novabiochem (San Diego, CA) and Advanced Chemtech (Louisville, KY). Ethanolamine and trifluoroethanol (TFE) were from Sigma-Aldrich (St. Louis, MO). Lipids were obtained from Avanti Polar Lipids (Alabaster, AL). Other chemicals were the highest grade available from EMD (Gibbstown, NJ).

Peptides (Table 1) were synthesized as described previously.[24] In some peptides, deuterium-labeled alanine-d_4 was incorporated at specific positions in the sequence, namely, in 100% abundance at a single residue or at 50−75% abundance at another sequence position, by combining appropriate amounts of Fmoc-Ala-d_4 and Fmoc-Ala in one vial. In other peptides, [^{15}N]Leu and [^{15}N]Ala were incorporated at 100% isotope abundance in particular sequence positions. The isotope-labeled amino acid positions are noted in the figure legends.

DLPC, DMPC, and DOPC bilayer membrane lipids were chosen to represent a range of fluid bilayers of differing hydrophobic thicknesses, ~19.5, ~23, and ~27 Å, respectively.[6,25] The double bond in the acyl chains of DOPC is necessary to maintain appropriate lipid bilayer fluidity at physiological temperature. While the lipid unsaturation also will influence the lateral pressure profile,[26] the influence of pressure or packing density appears to be rather minimal for the tilt angles of the types of helices considered here.[6]

Vesicle samples containing 0.13 μM peptide and 7.8 μM lipid for CD spectroscopy were prepared by sonication, as previously described.[7,27] Spectra were recorded using a Jasco (Easton, MD) J710 CD spectropolarimeter, scanning from 190 to 250 at a rate of 20 nm/min, using a 1 mm path length, a 0.2 nm step resolution, and a 1 nm bandwidth, with five scans averaged. (Because of far-UV absorption by the double bond in DOPC, samples in DOPC were scanned from 200 to 250 nm.) Samples for fluorescence spectroscopy were prepared by ~40-fold

Table 1. Sequences of Peptides[a]

C-anchored WALP	n=4[b]	a-ALALALALWWG-e
C-anchored WALP	n=8[b]	a-ALALALALALALALALWWG-e
N-anchored WALP	n=8[b]	a-GGWWLALALALALALALALA-e
N-anchored WALP	n=4[b]	a-GGWWLALALALA-e

[a]The abbreviations a and e denote acetyl and ethanolamide, respectively. Labels were incorporated for ^2H and ^{15}N NMR experiments, as indicated in Materials and Methods. [b]The integer n denotes the number of LA or AL dipeptide units in the sequence.

dilution of the samples used for CD spectroscopy. Intrinsic Trp emission spectra were recorded using a Perkin-Elmer LS 55 fluorescence spectrophotometer, at an excitation wavelength of 284 nm, detection of emission in the 300−500 nm range, and slits of 7.5 nm for both excitation and emission. Ten scans recorded at a rate of 200 nm/min were averaged.

Samples for NMR spectroscopy were prepared as described previously.[24] Glass plate samples had a peptide:lipid ratio of 1:40 and 45% hydration (w/w). Bicelle samples were prepared as described previously,[24] using DMPC with DH-o-PC or DM-o-PC with DH-o-PC (for the ^{15}N-labeled samples) in a molar ratio (q) of 3.2, and a ^{15}N-labeled peptide:DMPC ratio of 1:80. Solid-state deuterium NMR spectra were recorded[24] at 50 °C for the plate samples and 40 °C for the bicelle samples. High-resolution separated local field solid-state NMR spectra obtained utilizing the SAMPI4 pulse sequence[28,29] were obtained on a 500 MHz Bruker Avance spectrometer. Data were acquired using a 1 ms cross-polarization (CP) contact time and radio frequency (RF) field strengths of approximately 50 kHz; 54 t_1 points were acquired in the indirect dimension, with 8.0 ms of acquisition time in the direct (t_2) dimension, and a 7.5 s recycle delay. ^{31}P NMR spectra (Figure S1 of the Supporting Information) indicated that the lipids were well-aligned. Combinations of ^{2}H quadrupolar splitting magnitudes, along with ^{15}N chemical shift and ^{15}N−^{1}H dipolar coupling values, when available, were used to describe the orientations and dynamics of the peptides in the different lipid systems.[20] The methods for the semistatic and Gaussian treatments of the dynamics have been described previously.[20,24,30]

RESULTS

The desired peptides in Table 1 were successfully synthesized and characterized. Mass spectra (Figure S2 of the Supporting Information) confirmed the expected isotopic mass distributions for labeled peptides with full or partial deuteration of two alanines. HPLC chromatograms (Figure S3 of the Supporting Information) revealed single major peaks, indicating that the synthetic peptides were ∼95% pure.

The secondary structures of the membrane-incorporated peptides were examined by CD spectroscopy. The longer 19- or 20-residue peptides, with eight Leu-Ala units, yield CD spectra characteristic of α-helices in DLPC, DMPC, and DOPC (Figure 2). It is evident that the shorter lipids promote a larger extent of helix formation, perhaps because of better matching of the lipid and peptide hydrophobic lengths. The spectral differences could perhaps arise from partial helix unwinding in the longer lipids. We do not fully understand the reasons for these trends.

A much shorter 11-residue hydrophobic peptide, with Trp anchors at positions 9 and 10, which potentially could span a lipid monolayer as an α-helix, is not helical in any of the lipid bilayer membranes (Figure 2C). Instead, the shorter C-anchored peptide, with its $(LA)_4$ sequence, exhibits CD spectra characteristic of a β-sheet in each of the lipid membranes. The deuterium NMR spectra additionally suggest that this shorter peptide undergoes aggregation. Indeed, the spectra from hydrated, oriented DMPC bilayers with the 11-residue half-WALP peptides show a characteristic Pake powder pattern, recognized as a full range of quadrupolar splittings that reaches a maximum at ∼37 kHz (Figure 3E,F). The spectra are furthermore nearly identical for the β = 0° and β = 90° sample orientations, indicating slow motion of the peptide on the ^{2}H NMR time scale. The observed Pake patterns are likely a result

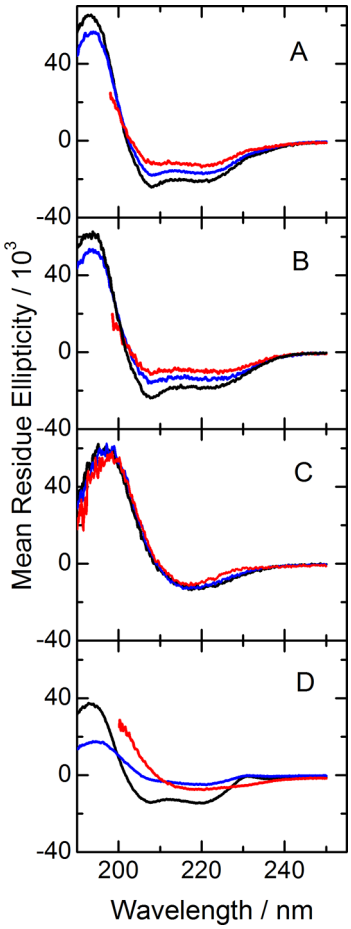

Figure 2. Circular dichroism spectra of N-anchored n = 8 (A), C-anchored n = 8 (B), C-anchored n = 4 (C), and N-anchored n = 4 (D) WALP peptides, in vesicles of DLPC (black), DMPC (blue), or DOPC (red). It is evident that the shorter lipids promote a larger extent of α-helix formation for the longer peptides.

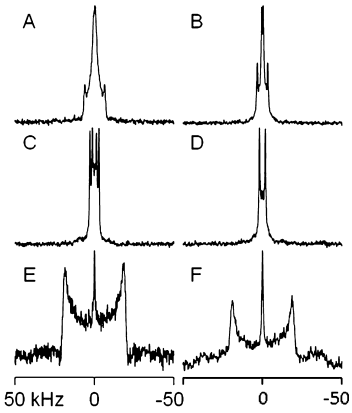

Figure 3. ^{2}H NMR spectra of labeled alanines in N-anchored n = 8 (A and B), C-anchored n = 8 (C and D), and C-anchored n = 4 (E and F) WALP peptides, in hydrated bilayers of DMPC oriented at β = 0° (A, C, and E) or β = 90° (B, D, and F), at 50 °C. The ^{2}H-labeled alanine residues and percent deuteration are $A^6_{70\%}$ and $A^8_{100\%}$ (A and B), $A^{13}_{70\%}$ and $A^{15}_{100\%}$ (C and D), or $A^3_{75\%}$, $A^5_{50\%}$, and $A^7_{100\%}$ (E and F).

of peptide aggregation. To address this issue, we synthesized a complementary N-anchored half-WALP peptide having again only four Leu-Ala units (Table 1). When the N- and C-anchored half-WALP peptides were incorporated together in

DMPC-oriented bilayer samples, in a 1:1 ratio (1:40 total peptide:lipid ratio), the resulting ^{2}H NMR spectra still remained as Pake patterns (Figure S4 of the Supporting Information). The preservation of the powder pattern indicates that the presence of the N-anchored half-WALP peptide does not prevent aggregation of the C-anchored half-WALP peptide. The N-anchored half-WALP peptide furthermore exhibits CD spectra that suggest mixed secondary structures, albeit with evidence of some helix formation in DLPC (Figure 2D).

The longer WALP-like peptides, with pairs of Trp anchors on only the C-terminus or only the N-terminus, and with hydrophobic lengths sufficient to span lipid bilayers, do adopt transmembrane helical configurations in oriented DLPC, DMPC, and DOPC lipid bilayers. The NMR spectra (Figure 3A–D) display sharp, resolved ^{2}H resonances for the pairs of labeled alanines (Figure 3A–D). Importantly, the narrow resonances and the factor of 2 reduction with the change in sample orientation from $\beta = 0°$ to $\beta = 90°$ indicate that these longer peptides undergo rapid motional averaging about the bilayer normal, in stark contrast to the aggregated shorter peptides that give essentially identical Pake patterns at $\beta = 0°$ and $\beta = 90°$ (Figure 3E,F). Full sets of ^{2}H NMR spectra for both sample orientations are included as Figures S4–S8 of the Supporting Information. The quadrupolar splittings measured from the NMR spectra are summarized in Table 2, for the $\beta =$ 0° and $\beta = 90°$ sample orientations. Where possible, prior to the analysis of peptide orientation, the ^{2}H $\Delta\nu_q$ magnitudes observed at $\beta = 90°$ were multiplied by 2 and averaged with the values observed at $\beta = 0°$.

Table 2. Observed ^{2}H Quadrupolar Splitting Magnitudes (kilohertz) for Labeled Alanine Methyl Groups in Half-Anchored WALP Peptides[a]

Ala[b]	DLPC	DMPC	bicelles[c]	DOPC
		N-Anchored WALP		
6	15.1	12.4	–	10.0
8	3.4	1.8	–	5.1
10	16.0	10.2	–	9.3
12	2.4	6.8	–	4.9
14	12.6	7.4	–	8.3
16	6.8	7.4	–	8.3
18	4.4	5.5	–	6.8
		C-Anchored WALP		
3	0.0	5.1	0.0	9.6
5	10.8	8.1	10.6	5.1
7	4.2	6.8	4.0	9.5
9	7.9	7.7	7.4	3.0
11	7.9	7.7	7.4	9.0
13	5.2	7.4	6.2	5.9
15	11.3	7.4	8.8	7.4

[a]Values for the $\beta = 0°$ sample orientation in the indicated lipid bilayers or in bicelles. Signals are from the CD_3 side chain. [b]Position of the alanine residue in the sequence. [c]Bicelles composed of DMPC and DH-o-PC ($q = 3.2$). Values left blank were not measured.

SAMPI4 solid-state NMR spectra were recorded for the bicelle-incorporated C-anchored $n = 8$ WALP peptide, labeled with ^{15}N at residues 5–15 (Figure 4A) or residues 11–15 (Figure 4B). The spectral patterns indicate an intermediate to large degree of peptide motion. Notably, the dispersion of the observed ^{15}N chemical shifts and ^{15}N–^{1}H dipolar couplings is much weaker than that observed with AG^{2}ALWLALALALA-

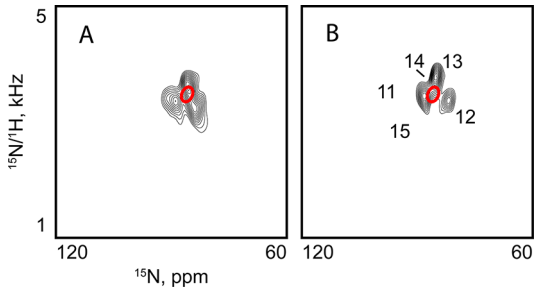

Figure 4. SAMPI4 spectra for C-anchored $n = 8$ WALP peptide with ^{15}N labels at residues 5–15 (A) or residues 11–15 (B). Peak assignments for labeled residues are shown in panel B. The PISA wheel patterns (red) are based on analysis of a combination of ^{2}H and ^{15}N data, with equal weights for the ^{2}H quadrupolar couplings, ^{15}N–^{1}H dipolar couplings, and ^{15}N chemical shifts.

LALALWLAG^{22}A (GWALP23)[20,30] yet conspicuously stronger than that observed for AW^{2}ALWLALALALALALALWLAW^{22}A ("WWALP23").[20] When five residues were labeled (Figure 4B), we could assign the magnitudes of the chemical shifts and dipolar couplings to specific residues. Assignments were based in part on the disposition of five consecutive residues in the framework of the helix geometry (Table 3),[24,30] and in part on the agreement with observed ^{2}H quadrupolar splittings for equivalent residues. When 11 residues were labeled (Figure 4A), the substantial peak overlap precluded the assignment of individual resonances.

Table 3. Dipolar Couplings and ^{15}N Chemical Shift Values for ^{15}N–^{1}H Groups in the C-Anchored ($n = 8$) WALP Peptide in DM-o-PC/DH-o-PC Bicelles ($q = 3.2$)[a]

residue	^{15}N–^{1}H dipolar coupling (kHz)	^{15}N chemical shift (ppm)
11	3.55	88.8
12	3.35	82.2
13	3.85	85.5
14	3.70	86.5
15	3.30	87.0

[a]Values are listed for bicelle samples, corresponding to a $\beta = 90°$ sample orientation.

The ^{2}H quadrupolar splittings for the $\beta = 0°$ sample orientation, with uncertainties of approximately ±0.5 kHz, were used to calculate the peptide average apparent tilt and direction of tilt (with respect to C_α of Gly^1).[4] Where available, the ^{15}N chemical shift and ^{15}N–^{1}H dipolar coupling values were also included. Molecular motions were treated in two ways, using either a semistatic approach, based on a single order parameter,[4] or a Gaussian dynamics approach,[16] based on the widths of distributions for the peptide tilt τ and helix azimuthal rotation ρ (defining the direction of tilt), expressed as σ_τ and σ_ρ, respectively. Results from both methods of analysis, using 7–17 data points, show substantial agreement and are summarized in Table 4.

The Gaussian and semistatic methods for treating the dynamics allowed us to estimate the helix orientations and dynamic properties in bilayer membranes of DLPC, DMPC, and DOPC, and in DMPC/DH-o-PC bicelles. The orientations are described by the average tilt magnitude τ_0 with respect to the bilayer normal and the average tilt direction (azimuthal rotation) ρ_0 with respect to C_α of Gly^1 (Table 4). The dynamics are expressed by means of a principal order parameter

dx.doi.org/10.1021/bi301394z | Biochemistry 2012, 51, 10066–10074

Table 4. Calculated Orientations of N- and C-Anchored WALP Peptides in Lipid Bilayers and Bicelles[a]

Trp position[b]	lipid	model	τ_0 (deg)	σ_τ (deg)	ρ_0 (deg)	σ_ρ (deg)	S_{zz}	rmsd (kHz)	n[c]
N-anchor	DLPC	Gaussian	13	18	201	60	0.88[d]	0.9	7
	DLPC	semistatic	7	na[e]	202	na[e]	0.75	0.9	7
	DMPC	Gaussian	7	15	180	76	0.88[d]	0.9	7
	DMPC	semistatic	3	na[e]	180	na[e]	0.78	0.9	7
	DOPC	Gaussian	3	15	193	60	0.88[d]	0.5	7
	DOPC	semistatic	2	na[e]	204	na[e]	0.78	0.8	7
C-anchor	DLPC	Gaussian	7	21	46	56	0.88[d]	0.5	7
	DLPC	semistatic	4	na[e]	46	na[e]	0.73	0.6	7
	DMPC	Gaussian	1	18	52	56	0.88[d]	0.4	7
	DMPC	semistatic	1	na[e]	60	na[e]	0.77	0.6	7
	bicelles	Gaussian	8	18	56	86	0.88[d]	0.9	17[f]
	bicelles	semistatic	3	na[e]	55	na[e]	0.74	0.9	17[f]
	DOPC	Gaussian	11	33	270	44	0.88[d]	0.6	7
	DOPC	semistatic	2	na[e]	285	na[e]	0.67	1.0	7

[a]The Gaussian model for the dynamics uses a fixed principal order parameter S_{zz},[16] representing the dynamic extent of (mis)alignment (angle α) between the molecular z-axis and its average orientation, characterized by the time average $S_{zz} = \langle 3\cos^2\alpha - 1\rangle/2$.[31] Within this context, further motions can be characterized by widths σ_τ and σ_ρ of Gaussian distributions about the average values of tilt magnitude τ_0 and tilt direction ρ_0.[16] An alternative semistatic analysis, using three parameters instead of four, determines the best fit (lowest rmsd) as a function of τ_0, ρ_0, and S_{zz}. [b]Each peptide has eight repeating Leu-Ala units. See sequences in Table 1. [c]The number of data points for the calculation is seven ^{2}H methyl quadrupolar couplings, unless otherwise noted. [d]Fixed value. [e]Not applicable. [f]In the DMPC/DH-o-PC bicelles (q = 3.2), the data points consisted of seven ^{2}H methyl quadrupolar couplings, five ^{1}H−^{15}N dipolar couplings, and five ^{15}N chemical shifts. Data points were weighted equally.

S_{zz} (semistatic) or the widths of Gaussian distributions σ_τ and σ_ρ. The rmsd values, typically ∼1.0 kHz, are in agreement with the precision of the experimental measurements. The Gaussian distributions σ_τ and σ_ρ were superimposed upon a fixed principal order parameter S_{zz} of 0.88, which is typical for representing an intrinsic molecular "wobble" for well-oriented systems.[1,31] The semistatic calculations converged to lower principal order parameters (S_{zz}) between 0.65 and 0.8, which reflect some motional properties of the peptides in the different lipid membranes (Table 4).

Both the N-anchored and C-anchored WALP peptides, each with eight Leu-Ala units, display small yet non-zero apparent average tilt angles in each of the lipid bilayer membranes (Table 4). While the precession entropy argues against a precisely zero tilt angle,[15] the estimates for τ_0 for all of the "single-anchored" peptide−lipid systems, as a group, fall within a narrow range of only 1−13°. As expected, and as observed generally with other systems,[20,32] when explicit parameters σ_τ and σ_ρ are considered, the Gaussian treatment of the peptide dynamics gives in most cases somewhat higher estimates of τ_0 than does a semistatic treatment with only a single variable, S_{zz} (Table 4). Even though one end of each peptide is without any obvious "anchor" residue, it is striking that in no case is τ_0 estimated to be zero, which again is disfavored by the precession entropy.[15] Indeed, if τ_0 would average to zero, then each of the alanine CD_3 quadrupolar splittings would average to the same value (see ref 4), but this is not the case, as is evident in the GALA wave plots (Figure 5).

As estimates of the helix motions, the deduced values of σ_τ and σ_ρ indicate substantial dynamics for each peptide in all of the lipid systems (Table 4). The best fits for σ_ρ are generally ∼60°, and the best fits for σ_τ are generally ∼20°. The minima in (σ_τ, σ_ρ) space are nevertheless shallow (Figure 6), indicating wide ranges of acceptable allowed combinations of (σ_τ, σ_ρ). As a corollary, the rather extensive peptide dynamics can be treated in a number of possible ways. If σ_τ and σ_ρ are not used, the (semistatic) variable S_{zz} falls into the range of 0.65−0.8

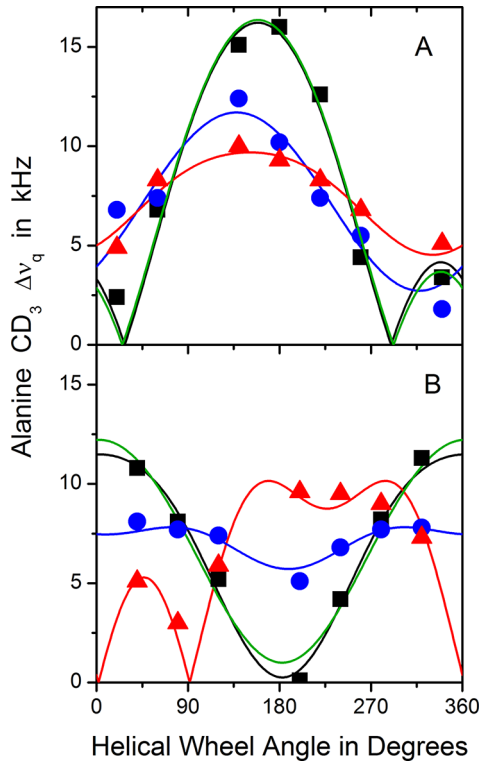

Figure 5. GALA quadrupolar wave plots for half-anchored n = 8 WALP peptides, with the paired Trp anchor residues that are N-proximal (A) or C-proximal (B). The curves represent the fits using Gaussian dynamics in the lipid environments of DLPC (black), DMPC (blue), or DOPC (red). For comparison, the semistatic fits are shown as green curves in DLPC.

(Table 4), again indicating considerable dynamics for the half-anchored bilayer-spanning peptides.

The most probable helix azimuthal rotation, which defines the direction of tilt ρ_0, does not depend upon which method is used to estimate the dynamics (Table 4). For the N-anchored

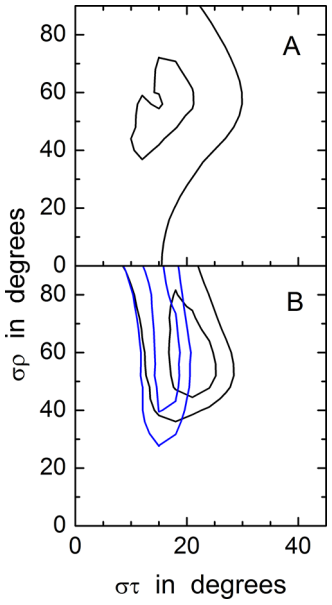

Figure 6. Gaussian dynamics. rmsd (σ_τ, σ_ρ) graphs for the Gaussian dynamics analysis of the n = 8 N-anchored (A) and C-anchored (B) WALP peptides in mechanically oriented bilayers of DLPC (black) or in magnetically oriented bicelles (blue). The contour levels are 1.0 and 2.0 kHz.

peptide, the preferred ρ_0 does not change much with the lipid bilayer thickness (Figure 7A), although, as expected, ρ_0 becomes essentially undefined as τ_0 approaches zero, namely in the thicker DOPC. Also for the C-anchored peptide, for very small values of τ_0, the distribution of probable ρ values (Figure 7B) becomes either bimodal (DOPC) or very flat (DMPC).

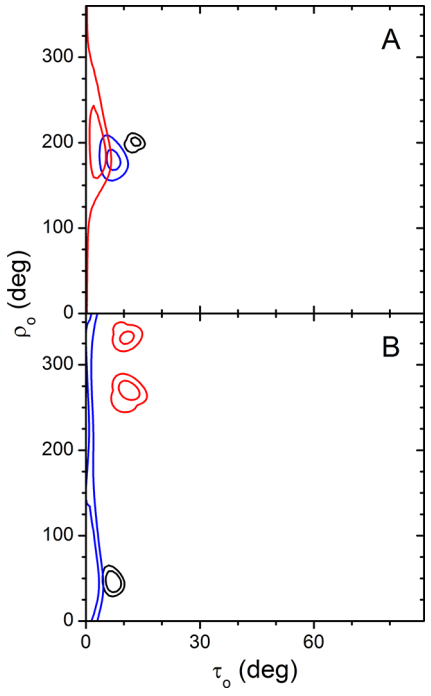

Figure 7. Orientations of half-anchored peptides. rmsd plots for the apparent tilt of the n = 8 N-anchored (A) and C-anchored (B) WALP peptides in oriented bilayers of DLPC (black), DMPC (blue), or DOPC (red). The rmsd is plotted as a function of τ and ρ values for the optimal values of σ_τ and σ_ρ in Gaussian calculations (see Table 4 and Figure 6). Contours are drawn at 1.2 and 2.0 kHz.

The results for the C-anchored peptide in the DMPC bilayer and the bicelle environments (Table 4) agree very closely, with just marginally (2−5°) higher estimates for τ_0 in the bicelles. Notably, the assessments of σ_τ and σ_ρ, or alternatively of the variable S_{zz}, to represent the dynamics, are nearly identical between the DMPC bilayers and bicelles. We note also that the bicelle results are based on combinations of 17 data points that include ^{15}N chemical shifts and ^{15}N−^{1}H dipolar couplings in addition to ^{2}H quadrupolar couplings. Nevertheless, the fitted PISA wheel patterns (Figure 4A) depend very little on whether the ^{15}N−^{1}H data are analyzed alone or in combination with ^{2}H data. In either case, the peptide dynamics and dispersion of resonances around the PISA wheel are intermediate between the cases of minimal (GWALP23) or very extensive (WWALP23) dynamic averaging of the NMR observables.[7,20]

The NMR experiments were complemented by measurements of the intrinsic Trp fluorescence spectra (Figure S9 of the Supporting Information). The emission maxima are 340 nm for the N-anchored (n = 8) WALP and 345 nm for the C-anchored (n = 8) peptide, compared to ∼351 nm, which is the expected value for Trp in an entirely aqueous environment. Each spectrum reports an average environment for the two Trp residues in a particular peptide. No change in λ_{max} with lipid thickness was observed for either of the peptides, suggesting that the pair of adjacent Trp residues on one side of the transmembrane helix may "float" to a preferred location within the bilayer−solution interface. The spectra suggest furthermore that the Trp residues of the N-anchored peptide, blue-shifted with respect to those of the C-anchored peptide, occupy average positions that are slightly more sequestered from the aqueous environment.

DISCUSSION

Traditional WALP peptides contain two Trp residues on either side of a Leu-Ala helical core of variable length, $(LA)_n$. Because the orientational preferences and motional behavior of the N- and C-terminal Trp residues can be different,[33] we developed peptides with two Trp residues on only one side of an $(LA)_n$ sequence that, because it is anchored on only one end, becomes effectively a "tail" sequence instead of a "core" sequence. The half-anchored WALP peptides of various lengths allowed us to address questions about the lipid interactions of the $(LA)_n$ tail sequences, including issues of secondary structure, aggregation behavior, potential for transmembrane topology, helix tilt, and dynamics. It is noteworthy that strikingly different behavior was observed for the shorter (n = 4) peptides as opposed to the longer (n = 8) peptides in lipid bilayer membranes.

For the shorter peptides with the $(LA)_4$ tail sequence, we observe neither a helical conformation nor a leaflet-spanning orientation. The results for a-ALALALALWWG-e and a-GGWWLALALALA-e (Table 1) are in agreement with the β-structure and aggregation observed previously for a-WLLLLL in POPC bilayer membranes.[34,35] Indeed, for the shorter $(LA)_4$ peptides, the CD spectra (Figure 2) indicate β-structure and the NMR spectra (Figure 3) indicate restricted motion, consistent with peptide aggregation. Consequently, for peptides that are too short to span a bilayer, in both the ALALALA-LWWG and WLLLLL families, it appears that the formation of β-structure is related to aggregation. Some sequence changes, for example, WLWLL, inhibit both the aggregation and the β-structure.[34] Longer $(AL)_n$ peptides that are able to adopt the

transmembrane topology, to span the bilayer, also fold into α-helices (Figure 2). Interestingly, correlations between secondary structure and protein aggregation furthermore relate to a variety of neurodegenerative diseases.[36−39]

The longer half-anchored WALP peptides, those with $(LA)_8$ core sequences, have hydrophobic lengths similar to that of WALP19 or WALP23[1,40] but are anchored to the lipid bilayer interface region on only one side. They incorporate into lipid bilayers as transmembrane helices and, unlike the shorter analogues, show no signs of aggregation. It is of interest to compare the average tilt and dynamics of uncharged transmembrane helices that possess either (a) two interfacial Trp residues on both ends,[4,7,9,17,32,41] (b) only one interfacial Trp on both ends,[6,7,20] or (c) two interfacial Trp residues on only one end (this work). These categories of transmembrane helical peptides have been examined in detail in bilayer membranes of different thicknesses, DOPC, DMPC, and DLPC.

When two interfacial Trp residues are present on both ends of a transmembrane helix, a prominent feature is extensive dynamic averaging of NMR observables,[9,14,20] which consequently do not change much with membrane thickness.[4,17,32] Remarkably, with fewer tryptophans, namely, only one Trp on each end of a core transmembrane helix, the dynamic averaging is reduced rather dramatically and the NMR observables show systematic variation with membrane thickness, such that the apparent helix tilt scales quite nicely with the membrane thickness.[6,7,20] A similar core helix flanked by a single Tyr and a single Trp shows a similarly low level of dynamic averaging;[27] nevertheless, the incorporation of just one more tyrosine on one end restores the extensive dynamic behavior.[27]

Within this context of single versus multiple interfacial aromatic residues flanking a central transmembrane helix, the half-anchored WALP peptides with the $(LA)_8$ tails introduce a new category. With one end now devoid of any aromatic residues, the result once again is dynamic averaging along with only small variations with membrane thickness. Indeed, the bilayer thickness dependence of the NMR observables—in DOPC, DMPC, and DLPC lipid bilayer membranes—appears to be similar to yet somewhat smaller than that of WALP23.[17] The scenario in which the half-anchored $(LA)_8$ WALP peptides are tilted very little and/or experience extensive motional averaging can be rationalized by both the lack of anchoring residues on one side and the multiple interfacial tryptophans on the other side of the lipid membrane. In any case, it is reasonable that, with one end "free", neither N-terminal nor C-terminal anchoring (alone) should be expected to generate a large helix tilt within a lipid bilayer. Interestingly, the most probable azimuthal rotation angle ρ_0 (defining the direction of tilt) in DLPC is roughly opposite for the C- and N-anchored $(LA)_8$-containing peptides. As anticipated, when the tilt magnitude approaches zero, the preferred azimuthal rotation defining the tilt direction becomes undefined (see Figure 7).

It is of particular interest to compare the dynamic behavior of a-ALALALALALALALALWWG-e (Figure 4) with that of a-AWALWLALALALALALALWLAWA-e (WWALP23).[20] Via comparison of the respective $^{15}N-^{1}H$ dipolar couplings and ^{15}N chemical shifts, it is apparent that ALALALALALALALALWWG exhibits intermediate dynamic behavior, between that of the highly dynamic WWALP23 and the much less dynamic AGALWLALALALALALALWLAGA (GWALP23). Indeed, for GWALP23, the backbone $^{15}N-^{1}H$ dipolar couplings and ^{15}N chemical shifts appear as fully dispersed individual resonances; for WWALP23, they collapse to a single peak,[20] and for ALALALALALALALALWWG, the backbone ^{15}N observables show the intermediate case of partial overlap (Figure 7). The dynamic properties of the membrane-spanning helices are regulated by the numbers and locations of interfacial tryptophan (and tyrosine) residues.

The results of the analysis of helix tilt in magnetically oriented DMPC/DH-o-PC bicelles and in mechanically oriented DMPC bilayers show close agreement (Table 4). Whether a combined analysis of deuterium and $^{15}N-^{1}H$ observables (17 data points) for the bicelles or an analysis of only the deuterium $\Delta\nu_q$ magnitudes (seven data points) for the bilayers is utilized, both systems yield values of 55−60° for σ_ρ and ∼18° for σ_τ, along with similar almost vanishingly small values for τ_0 (Table 4). For this example, therefore, the DMPC-based bilayer and bicelle systems yield results that are in agreement.

The WALP-like peptides having double Trp anchors on only one end provide new insights into the anchoring behavior of Trp residues and the importance of peptide hydrophobic length. The ^{2}H NMR and ^{15}N NMR experiments indicate small tilt angles and extensive dynamics for the longer bilayer-spanning helical peptides with the $(LA)_8$ tails. The properties of the N- and C-anchored peptides are similar. As expected, the direction of the peptide tilt becomes essentially undefined when the tilt magnitude becomes very small. The shorter half-WALP peptides with $(LA)_4$ tails form aggregates having β-type secondary structure.

■ ASSOCIATED CONTENT

Ⓢ Supporting Information

Additional NMR spectra, mass spectra, a chromatogram, and Trp fluorescence spectra. This material is available free of charge via the Internet at http://pubs.acs.org.

■ AUTHOR INFORMATION

Corresponding Author

*Address: 119 Chemistry Building, University of Arkansas, Fayetteville, AR 72701. Telephone: (479) 575-4976. Fax: (479) 575-4049. E-mail: rk2@uark.edu.

Funding

This work was supported in part by National Science Foundation Grant MCB 0841227 and by the Arkansas Biosciences Institute.

Notes

The authors declare no competing financial interest.

■ ACKNOWLEDGMENTS

We thank Patrick van der Wel, James Hinton, and Marvin Leister for helpful discussions. The peptide facility is supported by National Institutes of Health (NIH) Grants RR31154 and GM103429. The NMR facilities are supported by NIH Grant GM103450 and the Biotechnology Resource for NMR Molecular Imaging of Proteins at the University of California, San Diego, which is supported by NIH Grant P41EB002031.

■ ABBREVIATIONS

CD, circular dichroism; DH-o-PC, 1,2-di-*O*-hexylphosphatidylcholine; DLPC, 1,2-dilauroylphosphatidylcholine; DMPC, 1,2-dimyristoylphosphatidylcholine; DM-o-PC, 1,2-di-*O*-myristoylphosphatidylcholine; DOPC, 1,2-dioleoylphosphatidylcholine; Fmoc, fluorenylmethoxycarbonyl; GALA, geometric analysis of labeled alanines; MtBE, methyl-*tert*-butyl ether; PISEMA,

polarization inversion with spin exchange at magic angle; POPC, 1-palmitoyl-2-oleoylphosphatidylcholine; rmsd, root-mean-square deviation; TFA, trifluoroacetic acid.

REFERENCES

(1) Killian, J. A., Salemink, I., dePlanque, M. R. R., Lindblom, G., Koeppe, R. E., II, and Greathouse, D. V. (1996) Induction of nonbilayer structures in diacylphosphatidylcholine model membranes by transmembrane α-helical peptides: Importance of hydrophobic mismatch and proposed role of tryptophans. *Biochemistry 35*, 1037−1045.

(2) Schiffer, M., Chang, C. H., and Stevens, F. J. (1992) The functions of tryptophan residues in membrane proteins. *Protein Eng. 5*, 213−214.

(3) Doyle, D. A., Morais Cabral, J., Pfuetzner, R. A., Kuo, A., Gulbis, J. M., Cohen, S. L., Chait, B. T., and MacKinnon, R. (1998) The structure of the potassium channel: Molecular basis of K^+ conduction and selectivity. *Science 280*, 69−77.

(4) van der Wel, P. C. A., Strandberg, E., Killian, J. A., and Koeppe, R. E., II (2002) Geometry and intrinsic tilt of a tryptophan-anchored transmembrane α-helix determined by ^{2}H NMR. *Biophys. J. 83*, 1479−1488.

(5) de Planque, M. R., Boots, J. W., Rijkers, D. T., Liskamp, R. M., Greathouse, D. V., and Killian, J. A. (2002) The effects of hydrophobic mismatch between phosphatidylcholine bilayers and transmembrane α-helical peptides depend on the nature of interfacially exposed aromatic and charged residues. *Biochemistry 41*, 8396−8404.

(6) Vostrikov, V. V., and Koeppe, R. E., II (2011) Response of GWALP transmembrane peptides to changes in the tryptophan anchor positions. *Biochemistry 50*, 7522−7535.

(7) Vostrikov, V. V., Daily, A. E., Greathouse, D. V., and Koeppe, R. E., II (2010) Charged or aromatic anchor residue dependence of transmembrane peptide tilt. *J. Biol. Chem. 285*, 31723−31730.

(8) de Planque, M. R., Goormaghtigh, E., Greathouse, D. V., Koeppe, R. E., II, Kruijtzer, J. A., Liskamp, R. M., de Kruijff, B., and Killian, J. A. (2001) Sensitivity of single membrane-spanning α-helical peptides to hydrophobic mismatch with a lipid bilayer: Effects on backbone structure, orientation, and extent of membrane incorporation. *Biochemistry 40*, 5000−5010.

(9) Ozdirekcan, S., Etchebest, C., Killian, J. A., and Fuchs, P. F. (2007) On the orientation of a designed transmembrane peptide: Toward the right tilt angle? *J. Am. Chem. Soc. 129*, 15174−15181.

(10) Vostrikov, V. V., Grant, C. V., Daily, A. E., Opella, S. J., and Koeppe, R. E., II (2008) Comparison of "Polarization inversion with spin exchange at magic angle" and "geometric analysis of labeled alanines" methods for transmembrane helix alignment. *J. Am. Chem. Soc. 130*, 12584−12585.

(11) Vostrikov, V. V., Hall, B. A., Greathouse, D. V., Koeppe, R. E., II, and Sansom, M. S. (2010) Changes in transmembrane helix alignment by arginine residues revealed by solid-state NMR experiments and coarse-grained MD simulations. *J. Am. Chem. Soc. 132*, 5803−5811.

(12) Sparr, E., Ash, W. L., Nazarov, P. V., Rijkers, D. T., Hemminga, M. A., Tieleman, D. P., and Killian, J. A. (2005) Self-association of transmembrane α-helices in model membranes: Importance of helix orientation and role of hydrophobic mismatch. *J. Biol. Chem. 280*, 39324−39331.

(13) Holt, A., Koehorst, R., Rutters-Meijneke, T., Gelb, M., Rijkers, D., Hemminga, M. A., and Killian, J. A. (2009) Tilt and rotation angles of a transmembrane model peptide as studied by fluorescence spectroscopy. *Biophys. J. 97*, 2258−2266.

(14) Esteban-Martin, S., and Salgado, J. (2007) The dynamic orientation of membrane-bound peptides: Bridging simulations and experiments. *Biophys. J. 93*, 4278−4288.

(15) Lee, J., and Im, W. (2008) Transmembrane helix tilting: Insights from calculating the potential of mean force. *Phys. Rev. Lett. 100*, 018103.

(16) Strandberg, E., Esteban-Martin, S., Salgado, J., and Ulrich, A. S. (2009) Orientation and dynamics of peptides in membranes calculated from ^{2}H-NMR data. *Biophys. J. 96*, 3223−3232.

(17) Strandberg, E., Ozdirekcan, S., Rijkers, D. T., van der Wel, P. C., Koeppe, R. E., II, Liskamp, R. M., and Killian, J. A. (2004) Tilt angles of transmembrane model peptides in oriented and non-oriented lipid bilayers as determined by ^{2}H solid-state NMR. *Biophys. J. 86*, 3709−3721.

(18) Wang, J., Denny, J., Tian, C., Kim, S., Mo, Y., Kovacs, F., Song, Z., Nishimura, K., Gan, Z., Fu, R., Quine, J. R., and Cross, T. A. (2000) Imaging membrane protein helical wheels. *J. Magn. Reson. 144*, 162−167.

(19) Marassi, F. M., and Opella, S. J. (2000) A solid-state NMR index of helical membrane protein structure and topology. *J. Magn. Reson. 144*, 150−155.

(20) Vostrikov, V. V., Grant, C. V., Opella, S. J., and Koeppe, R. E., II (2011) On the combined analysis of ^{2}H and ^{15}N/^{1}H solid-state NMR data for determination of transmembrane peptide orientation and dynamics. *Biophys. J. 101*, 2939−2947.

(21) Kim, T., Jo, S., and Im, W. (2011) Solid-State NMR Ensemble Dynamics as a Mediator between Experiment and Simulation. *Biophys. J. 100*, 2922−2928.

(22) Percot, A., Zhu, X. X., and Lafleur, M. (1999) Design and characterization of anchoring amphiphilic peptides and their interactions with lipid vesicles. *Biopolymers 50*, 647−655.

(23) ten Kortenaar, P. B. W., Van Dijk, B. G., Peeters, J. M., Raaben, B. J., Adams, P. J. H. M., and Tesser, G. I. (1986) Rapid and efficient method for the preparation of Fmoc-amino acids starting form 9-fluorenylmethanol. *Int. J. Pept. Protein Res. 27*, 398−400.

(24) Rankenberg, J. M., Vostrikov, V. V., DuVall, C. D., Greathouse, D. V., Koeppe, R. E., II, Grant, C. V., and Opella, S. J. (2012) Proline kink angle distributions for GWALP23 in lipid bilayers of different thicknesses. *Biochemistry 51*, 3554−3564.

(25) de Planque, M. R. R., Greathouse, D. V., Koeppe, R. E., Schafer, H., Marsh, D., and Killian, J. A. (1998) Influence of lipid/peptide hydrophobic mismatch on the thickness of diacylphosphatidylcholine bilayers. A ^{2}H NMR and ESR study using designed transmembrane α-helical peptides and gramicidin A. *Biochemistry 37*, 9333−9345.

(26) Binder, H., and Gawrisch, K. (2001) Effect of unsaturated lipid chains on dimensions, molecular order and hydration of membranes. *J. Phys. Chem. B 105*, 12378−12390.

(27) Gleason, N. J., Vostrikov, V. V., Greathouse, D. V., Grant, C. V., Opella, S. J., and Koeppe, R. E., II (2012) Tyrosine replacing tryptophan as an anchor in GWALP peptides. *Biochemistry 51*, 2044−2053.

(28) Nevzorov, A. A., and Opella, S. J. (2003) A "magic sandwich" pulse sequence with reduced offset dependence for high-resolution separated local field spectroscopy. *J. Magn. Reson. 164*, 182−186.

(29) Nevzorov, A. A., and Opella, S. J. (2007) Selective averaging for high-resolution solid-state NMR spectroscopy of aligned samples. *J. Magn. Reson. 185*, 59−70.

(30) Gleason, N. J., Greathouse, D. V., and Koeppe, R. E., II (2011) Using Tyrosine to Anchor a Transmembrane Peptide. *Biophys. J. 100*, 635a−636a (abstract).

(31) Pulay, P., Scherer, E. M., van der Wel, P. C. A., and Koeppe, R. E. (2005) Importance of tensor asymmetry for the analysis of ^{2}H NMR spectra from deuterated aromatic rings. *J. Am. Chem. Soc. 127*, 17488−17493.

(32) Strandberg, E., Esteban-Martin, S., Ulrich, A. S., and Salgado, J. (2012) Hydrophobic mismatch of mobile transmembrane helices: Merging theory and experiments. *Biochim. Biophys. Acta 1818*, 1242−1249.

(33) van der Wel, P. C., Reed, N. D., Greathouse, D. V., and Koeppe, R. E., II (2007) Orientation and motion of tryptophan interfacial anchors in membrane-spanning peptides. *Biochemistry 46*, 7514−7524.

(34) Wimley, W. C., Hristova, K., Ladokhin, A. S., Silvestro, L., Axelsen, P. H., and White, S. H. (1998) Folding of β-sheet membrane proteins: A hydrophobic hexapeptide model. *J. Mol. Biol. 277*, 1091−1110.

(35) Wimley, W. C., and White, S. H. (2004) Reversible unfolding of β-sheets in membranes: A calorimetric study. *J. Mol. Biol. 342*, 703–711.
(36) Bates, G. (2003) Huntingtin aggregation and toxicity in Huntington's disease. *Lancet 361*, 1642–1644.
(37) Fawzi, N. L., Yap, E. H., Okabe, Y., Kohlstedt, K. L., Brown, S. P., and Head-Gordon, T. (2008) Contrasting disease and nondisease protein aggregation by molecular simulation. *Acc. Chem. Res. 41*, 1037–1047.
(38) Carulla, N., Zhou, M., Giralt, E., Robinson, C. V., and Dobson, C. M. (2010) Structure and Intermolecular Dynamics of Aggregates Populated during Amyloid Fibril Formation Studied by Hydrogen/Deuterium Exchange. *Acc. Chem. Res. 43*, 1072–1079.
(39) Stanley, C. B., Perevozchikova, T., and Berthelier, V. (2011) Structural formation of huntingtin exon 1 aggregates probed by small-angle neutron scattering. *Biophys. J. 100*, 2504–2512.
(40) de Planque, M. R. R., Kruijtzer, J. A. W., Liskamp, R. M. J., Marsh, D., Greathouse, D. V., Koeppe, R. E., de Kruijff, B., and Killian, J. A. (1999) Different membrane anchoring positions of tryptophan and lysine in synthetic transmembrane α-helical peptides. *J. Biol. Chem. 274*, 20839–20846.
(41) Holt, A., Rougier, L., Reat, V., Jolibois, F., Saurel, O., Czaplicki, J., Killian, J. A., and Milon, A. (2010) Order parameters of a transmembrane helix in a fluid bilayer: Case study of a WALP peptide. *Biophys. J. 98*, 1864–1872.